Medical Engineering and Physics 37 (2015) 892–897

Contents lists available at ScienceDirect

Medical Engineering and Physics

journal homepage: www.elsevier.com/locate/medengphy

Technical note

Design and testing of a high-speed treadmill to measure ground reaction forces at the limit of human gait

Matthew W. Bundle[a,*], Michael O. Powell[a], Laurence J. Ryan[b]

[a] Biomechanics Laboratory, Department of Health and Human Performance, University of Montana, Missoula, MT 59812, USA
[b] Locomotor Performance Laboratory, Department of Applied Physiology and Wellness, Southern Methodist University, 5538 Dyer Street, Dallas, TX 75206, USA

ARTICLE INFO

Article history:
Received 16 October 2014
Revised 27 January 2015
Accepted 25 April 2015

Keywords:
Instrumented treadmill
Human gait
Sprint running

ABSTRACT

Investigations focused on the gait and physiological limits of human speed have been on-going for more than a century. However, due to measurement limitation a kinetic understanding of the foot-ground collision and how these dynamics differ between individuals to confer speed and limit gait has only recently begun to come forth. Therefore, we designed and tested an instrumented high-speed force treadmill to measure the forces occurring at the limits of human performance. The treadmill was designed to maximize flexural stiffness and natural frequency by using a honeycomb sandwich panel as the bed surface and a flexible drive shaft between the drive roller and servo motor to reduce the mass of the supported elements which contribute to the system's response frequency. The functional performance of the force treadmill met or exceeded the measurement criteria established for ideal force plates: high natural frequency (z-axis = 113 Hz), low crosstalk between components of the force ($F_x/F_z = 0.0020$[SD = 0.0010]; $F_y/F_z = 0.0016$[SD = 0.0003]), a linear response ($R^2 > 0.999$) for loading with known weights (range: 44–3857 N), and an accuracy of 2.5[SD = 1.7] mm and 2.8[SD = 1.5] mm in the x and y-axes, respectively, for the point of force application. In dynamic testing at running speeds up to 10 m s^{-1}, the measured durations and magnitudes of force application were similar between the treadmill and over-ground running using a force platform. This design provides a precise instrumented treadmill capable of recording multi-axis ground reaction forces applied during the foot ground contacts of the fastest men and animals known to science.

1. Introduction

The use of instrumented treadmills to measure the ground reaction forces produced during the foot ground contacts of human walkers and runners has become wide spread in both clinical and scientific settings. These devices substantially enhance both the quality and quantity of kinetic data obtained from the assessment of steady-speed walking and running by reducing the variability of within stride parameters and by substantially reducing subject time commitments and the research personnel effort compared to the use of in-ground force platforms. Because the patterns of force application and the timing of foot ground collisions vary between walking and running, treadmills designed to study the different gaits require separate engineering solutions [e.g. 1,2]. Similarly, during high-speed running the brevity of the foot-strike and the magnitude of the forces applied also require distinct engineering considerations. As a result, multi-axis ground reaction force data, from high speed treadmill running has, at present, come forth from only one laboratory [3]. One other group [4] and the study reporting the fastest speed yet observed [11.1 m s^{-1}; 5] have reported the vertical waveforms during treadmill sprinting at speeds greater than 8.0 m s^{-1}. The response characteristics and mechanical properties of these instruments have not been described in the literature. Here, we provide the design and testing of a custom, instrumented, force treadmill that is capable of measuring the forces applied in the vertical and horizontal axes and of achieving belt speeds that are faster than the current human speed record; currently 12.3 m s^{-1} [6].

Studies focused on the gait mechanics used during high-speed running have observed foot ground contacts as brief as 0.080 s [7] and peak ground reaction forces up to 5 times the individual's body weight [3], corresponding to roughly 4000 N. These durations and forces are essentially one-third as brief and 100% greater, respectively, than those observed at the lesser running speeds that are typically used while studying human gait [e.g. 1,2,8,9]. Due to the substantial impulses, a high system fundamental frequency is needed in order to faithfully transmit the applied forces to the force transducers. The most rapid events within the ground reaction force waveform occur with an interval of 0.020 s, and these waveforms can be adequately reproduced ($R^2 > 0.99$) by a Fourier series incorporating terms up to

* Corresponding author. Tel.: +1 406 243 4582; fax: +1 406 243 6252.
E-mail addresses: matt.bundle@mso.umt.edu (M.W. Bundle), mopowell@ucsc.edu (M.O. Powell), lryan@mail.smu.edu (L.J. Ryan).

http://dx.doi.org/10.1016/j.medengphy.2015.04.009
1350-4533/

75 Hz [5]. Generally, the natural frequency of a suspended structure such as a treadmill bed is enhanced by minimizing the mass of the supported material and by augmenting its intrinsic stiffness (Eq. (1)). A potential design strategy therefore, would be to reduce the dimensions of the supported surface, however, in order to test runners at the limits of human speed, the treadmill bed must be at least 1.7 m in length to accommodate the displacement of the foot during ground contact [10].

Existing instrumented force treadmills have been created by installing force platforms within the bed surface [11], mounting commercial or custom treadmills on top of in-ground force platforms [1,12,13] or force transducers [4,14,15,16,17], or have used proprietary techniques [3,5]. Force treadmills with an internal force platform are able to measure the vertical component of the ground reaction force only. Whereas, designs using the mount-on-top solution are able to detect the forces applied in multiple axes, because the internal frictional forces within the device cancel, only the forces applied by the leg contribute to the sum of forces that are measured by the transducers [17]. However, this design requires the mass of the entire apparatus to be supported by the transducers, otherwise an unknown amount of force may be dissipated through the non-instrumented support. In some designs the supported treadmill elements include a flywheel for belt-speed maintenance, the mass of which further reduces the response frequency of the system. On the basis of these findings and the recognition of the considerably more difficult instrumentation challenge present in a high speed application we excluded existing designs due to concerns of measurement capability.

Therefore, we modified the mount-on-top strategy, and used a sandwich structured composite with a honeycomb core to achieve high strength per unit weight for the bed surface, and reduced the mass of the supported treadmill elements by using a flexible drive shaft to prevent the servo motor's mass from contributing to the natural frequency of the system. In addition, we minimized system mass wherever possible in the design stage by using light weight components in the fabrication and drive system. We established as a target a fundamental frequency of 90 Hz, thereby providing a small margin of error in order to ensure the actual fundamental frequency exceeded the 75 Hz minimum [5] required for the system to faithfully transmit the applied dynamic forces to the load cells for direct measure. We evaluated the functional performance of the treadmill in accordance with the objective measurement criteria established previously [18,19] for ideal force plates namely, low crosstalk between the measured components of the force and a linear response with sufficient sensitivity over the range of anticipated dynamic forces. Finally, we evaluated the precision of the treadmill's ability to determine the point of force application across the bed's surface.

2. Materials and methods

2.1. Design

To achieve our goal of a 90 Hz natural frequency for the treadmill system, we undertook the following modeling procedure. We approximated the natural frequency in accordance with:

$$\text{Natural frequency (Hz)} = \frac{1}{2\pi}\sqrt{\frac{P}{\delta m}}, \tag{1}$$

where P is the maximum force we expected to observe during sprint running, δ is the vertical deflection resulting from P, and m is the mass of the supported equipment. We anticipated that peak ground reaction forces would remain less than 5000 N. These are roughly the forces that would allow a 100 kg runner to apply elite sprinter levels of peak force. This overestimates the likely observed forces because this body mass is roughly 25% greater than the typical elite level sprinter [20].

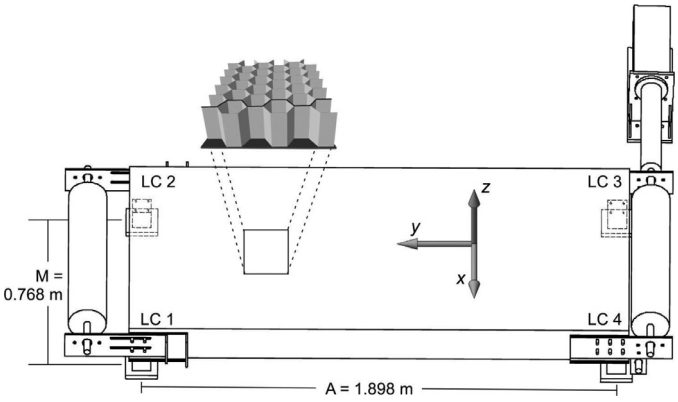

Fig. 1. A component diagram of the high-speed force treadmill and the locations of the load cells (LC). The M and A constants are used to determine the point of force application in accordance with Eqs. (3) and (4). The flexible line shaft connecting the motor to the rear axle permits the removal of the motor's mass from the elements contributing to the treadmill system's natural frequency. Inset illustrates the corrugated foil (black line), or ribbon, within the sandwich panel, this orientation produces a 2-fold higher stiffness in the y vs x axis. For clarity, the decking surrounding the treadmill and the safety harness worn by the subjects are not shown.

To estimate the vertical deflection under load we used simply-supported, centrally-loaded, beam theory equations designed for sandwich structures, as described by Hexcel [21]:

$$\delta = \frac{2k_b P l^3}{E_f t_f h^2 b} + \frac{k_s P l}{bhG_c} \tag{2}$$

where k_b is the beam-bending deflection coefficient ($k_b = \frac{1}{48}$), l is the length of the treadmill bed, k_s is the beam-shear deflection coefficient ($k_s = \frac{1}{4}$), E_f is the modulus of elasticity of the facing skin, h is the height of the honeycomb core, t_f is the thickness of the facing skin, b is the width of the treadmill bed, and G_c is the shear modulus of the core in the direction of the applied load. We selected a bed length of 2.00 m to provide 0.30 m of additional space for foot placement and be able to accommodate an expected 1.7 m of travel by the foot during ground contacts at speeds approaching the current human limit [6,10].

We used an iterative optimization approach that maximized vertical stiffness to determine the internal properties of the honeycomb panel. Finite element analysis (Autodesk Inventor, CA, USA) provided estimates of the response of the honeycomb laminate to loading by a virtual model that matched the dimensions of the human forefoot (63 mm × 77 mm). An aluminum (alloy 3003) honeycomb core with 6.35 mm cell sizes, and a density of 83.3 kg m^{-3}, permanently bonded to a 3.175 mm thick aluminum (alloy 5052) facing skin and loaded as above provided a compression safety factor of 3, and a single cell dimpling safety factor of 15. Increased distance between the facing skins acts to reduce the vertical deflection of a panel (Eq. (2)), however in North America non-custom orders of honeycomb are limited to the 15.24 cm height we used. Finally, within the plane of a honeycomb panel, the panel is 2-fold stiffer [21] in the axis parallel to the direction of the ribbons of material forming the core, here the ribbon direction is parallel to the y-axis (Fig. 1).

To further reduce the supported mass we used a flexible line shaft (R+W Coupling Technology, IL, USA—ZA 150) to remove the motor from the total supported mass of the bed system. The purpose of the coupling was to permit a rigid mounting of the motor to the floor and allow the instrumented bed to move independently, thus preventing the motor from dissipating loads applied to the bed. According to the manufacturer the load cells (AMTI, MC3A; MA, USA) have a stiffness of 3.0 × 10^8 N m^{-1} providing an expected maximum deflection of 0.017 mm for the specifics of our assembly (Fig. 1); well within the 5.8 mm of misalignment tolerated by the line shaft without resistive forces.

This modeling approach and these dimensions provided an a priori natural frequency estimate in the z-axis of 85 Hz. A second, and related method, provided a z-axis estimate of 91 Hz [22], this alternate procedure uses a modification of Eq. (2) that incorporates Poisson's ratio. We considered these to be conservative minimums for the final system because of the improved stiffness gained by rigidly mounting the bed on the load cells.

2.2. Motion control

The intermittent nature of force application during human running requires a motor capable of delivering large peak torques within the very brief periods of foot-ground contact when the load is applied. We used a servo controlled, 3-phase, 230 V, AC motor (Baldor Electric Company, BSM100C-6150-AA; AR, USA), that is capable of supplying 90 N m of peak torque and accepting 61.3 A of peak current. The motor is controlled by a servo drive (Baldor Electric Company, Flex+Drive-II) with a peak current rating of 55 A. The drive receives user issued commands from a personal computer via the serial port.

The treadmill belt is 2.2 mm thick and weighs 2.5 kg/m^2, it has a PVC coating overlying a polyester fabric weave (Forbo Siegling, Transilon: E 8/2 0/V5H S/MT). We reduced friction between the belt and the treadmill surface by applying a silicone fluid with a viscosity of 50 cSt (Clearco Products, Bensalem PA). This fluid coats the aluminum surface of the honeycomb panel and acts to reduce the magnitude of the instantaneous torques necessary from the servo motor.

2.3. Data acquisition and signal analysis

The x, y, z force signals (Fig. 1) from each of the load cells were amplified (AMTI, MSA-6; MA, USA), and digitized (Axon Instruments Inc., Digidata 1322A; CA, USA) at 2000 Hz prior to being saved to a personal computer. These signals were protected from electromagnetic interference emitted by the motor and power supply by placing 14 cm of ferrite beading on each end of the data and power cables. The individual load cell analog force signals were calibrated in accordance with the manufacturers specifications and then processed (WaveMetrics Inc., Igor Pro 6.34A; OR, USA) with a dual pass of a 6-pole, low pass, Butterworth filter producing a zero-lag filter with an effective cutoff frequency of 40 Hz [23]. The filtered waveforms were then summed to generate the x, y, z components of the ground reaction force.

The x and y locations of the point of force application, also called the center of foot-ground pressure, were determined in accordance with:

$$\mathrm{CoP}_x = \frac{M\,(F_{z1} + F_{z4})}{\sum_1^4 F_z} \tag{3}$$

and

$$\mathrm{CoP}_y = \frac{A\,(F_{z1} + F_{z2})}{\sum_1^4 F_z} \tag{4}$$

where M is the distance between the left and right (x-axis) transducers (0.768 m), A is the distance between the rear and front (y-axis) transducers (1.898 m), F_z is the vertical force measured by the load cell identified by the numerical subscript (Fig. 1), and $\sum_1^4 F_z$ is the sum of F_z from the 4 transducers [15]. The CoP_x and CoP_y measures obtained from Eqs. (3) and (4) were then transformed from an origin at the center of the third load cell (Fig. 1) to the treadmill coordinate system origin.

2.4. Testing

2.4.1. Natural frequency

The natural frequency of the force treadmill system was measured by modifying the method of Kram et al. [1]. Here we analyzed the impulsive response of the x, y, z components of the GRF created by striking the treadmill in each axis with a wooden ball (mass = 18.30 g; diameter = 37.9 mm). We performed a fast Fourier transform (FFT) on the parallel raw force signal from each impact after signal conditioning with a 60 Hz notch filter. We defined the natural frequency as the value corresponding to the peak of the first harmonic of the frequency spectrum.

2.4.2. Flexible drive shaft

To test if force was dissipated to the ground via the flexible line shaft connecting the motor to the rear axle, we placed the motor on a force plate (Bertec Corporation, 4060; OH, USA) and loaded the treadmill bed (range = 198–1778 N). During these tests we simultaneously recorded the forces detected by the treadmill load cells, and those dissipated to the force plate via the line shaft and motor. We tested force dissipation in a single axis because the line shaft is radially symmetrical and is capable of equal displacements (5.8 mm) throughout the 360° range of motion possible the YZ-plane.

2.4.3. Force detection and crosstalk

The ability to detect vertical loading and the computation of the mechanical crosstalk from an F_z load onto the x and y axes was determined by placing 16 known loads (range = 44–3857 N) on the center of the treadmill surface. The crosstalk was evaluated as the fraction of the vertical force that was detected by the horizontal elements of the load cells and expressed as a percentage in accordance with $(F_x/F_z) \times 100$ and $(F_y/F_z) \times 100$.

2.4.4. Precision of the CoP

A grid of 13 rows by 5 columns with vertices spaced at 15 cm increments was applied to the surface of the bed. The Cartesian positions of the vertices were verified by digitizing four different calibrated image views of the grid using the software and method of Hedrick [24]. We placed a dead weight (20.25 kg) above a 4 mm diameter stylus that was moved to each of the 65 locations marked by the grid. This permitted a comparison of the x and y differences between the digitized point locations and the center of pressure determined from the treadmill force sensors and computed in accordance with Eqs. (3) and (4).

2.4.5. Comparison to over-ground running

Two young healthy male sprinters provided written informed consent in accordance with the guidelines of the institutional review board at the University of Montana. The runners performed top speed runs over two in-ground force platforms (Bertec Corporation, 4060; OH, USA), that were located at the end of a 40 m runway. The maximum over-ground speed was determined from the time elapsed between two voltage pulses emitted in response to the interruption of infrared photocell beams (Banner Engineering, SM912LV; MN, USA) placed 3.0 m apart, surrounding the in-ground force plates, at a height of 1.15 m [25].

The treadmill testing was conducted by performing a discontinuous speed incremented series of trials up to the speed matching the maximum over-ground speed attained using the procedure of Weyand et al. [26].

3. Results

3.1. Natural frequency

The natural frequencies of the force treadmill system obtained from the FFT of the force recordings from impacts of a wooden ball striking the treadmill bed in each of the component axes were; 166 Hz in the x-axis, 168 Hz in the y-axis, and 113 Hz in the z-axis.

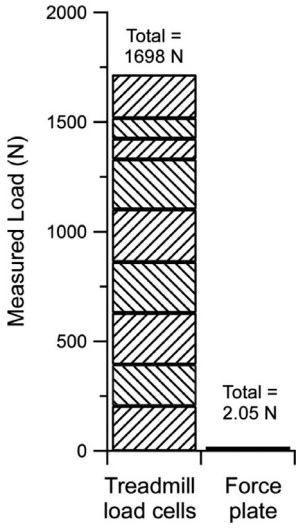

Fig. 2. We applied 9 loads to the treadmill surface and simultaneously measured the force dissipated by the line shaft while the motor rested on a force platform (range: 198–1778 N). The maximum force measured by the force platform was 2.1 N when the force treadmill registered a load of 1698 N.

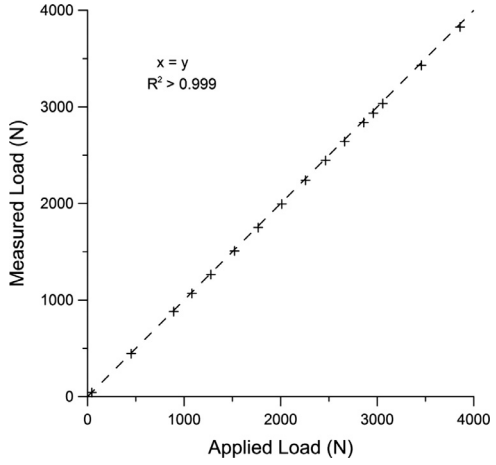

Fig. 3. The results of a 16 point calibration test of loads placed on the center of the treadmill bed (range: 44–3857 N). When the measured values were fit with the line of identity (i.e. $y = x$), the regression coefficient was greater than 0.999. With treadmill measurements matched the applied load to within 0.94 (SD = 0.38)%.

3.2. Flexible drive shaft

The mean vertical force dissipated from the bed via the flexible line shaft and the motor was 0.15% ± 0.079% of the 9 applied static loads (Fig. 2). In absolute terms, the greatest force measured by the force plate was 2.1 N when the force treadmill registered a load of 1698 N.

3.3. Force detection and crosstalk

The relationship between the weight applied to the surface of the treadmill bed and vertical reaction force measured by the load cells was highly linear (Fig. 3). When the measured values were fit with the line of identity (i.e. $y = x$), the 16 loads applied generated a regression coefficient that was greater than 0.999, with an average difference of 0.94 (SD = 0.38)%. The mechanical crosstalk terms exerted in the x and y axes from a load applied in the z-axis were 0.20 (SD = 0.10)% in the x and 0.16 (SD = 0.03)% in the y. The maximum force detected in x and y was 2.97 N and 3.32 N, respectively, when loaded with 3857 N of deadweight.

3.4. Center of pressure

The average difference values between the 65 grid vertices and the points of force application determined from Eqs. (3) and (4) were 2.5 (SD = 1.7) mm in the x and 2.8 (SD = 1.5) mm in the y.

3.5. Comparison to over-ground running

The stance forces and durations of foot ground contact were similar between the over-ground and treadmill sprints for the two subjects who completed this testing (Fig. 4). For both subjects, the force plate obtained measures of stance average ground reaction force, peak vertical force (z-axis), and durations of foot ground contact (T_c) were within 1 standard deviation of the means obtained from trials administered at the same speed but on the force treadmill. Specifically, for subject 1, at his top speed of 8.1 m s^{-1}, the force plate vs treadmill data were: GRF_{avg}: 1428 vs 1459 (SD = 77) N, $F_{z\text{-peak}}$: 2743 vs 2464 (SD = 284) N, T_c: 0.123 vs 0.120 (SD = 0.005) s. For the second subject, at his top speed of 9.8 m s^{-1}, the force plate vs treadmill data were: GRF_{avg}: 1724 vs 1774 (SD = 108) N, $F_{z\text{-peak}}$: 2644 vs 2944 (SD = 364) N, T_c: 0.114 vs 0.109 (SD = 0.006) s.

4. Discussion

During the testing procedures performed, the high-speed force treadmill produced through this design provided highly accurate measures of both force application and point of force location (CoP). Our efforts to optimize flexural stiffness of the bed, in order to achieve a system natural frequency sufficient to resolve the most rapidly occurring elements of the reaction force waveform were successful. The modeling approaches for simply supported attachment, and the honeycomb composite material property expectations used in the design of the treadmill bed provided a conservative estimate of the empirical measures obtained from the final rigid installation. In the current application we observed a 30% increase in system frequency response compared to our a priori expectations, likely due to the conservative assumptions of simply supported loading. When combined with our initial over-engineered design, the final system frequency is 51% greater than the highest frequency term of a Fourier series known [5] to adequately reproduce the vertical ground reaction waveform.

A primary factor responsible for the high response frequency of the treadmill system was the removal of the motor's mass from the portion supported by the load cells. Under direct testing the flexible line shaft that permitted this design dissipated 0.15 ± 0.079% of the loads detected by the force treadmill. Moreover, at sprinting speeds up to nearly 10 m s^{-1} the torsional stiffness of the shaft has been able to adequately transmit the high instantaneous torques delivered by the servo motor to overcome the resistance of the foot ground collisions. In these experiments, ground contacts were measured to be as brief as 0.098 s with a peak vertical force of 3876 N.

Several of our static testing results can be directly compared to those of five other instrumented treadmills that have been designed, at least in part, to study the running gait [1,15,27,28,29]. When loaded up to 3857 N (comparison μ = 785 N; max = 2300 N) the relation between the weight applied to the treadmill surface and the forces measured from the load cells was highly linear, with an average deviation of 0.94 % (comparison μ = 1.30%; min = 0.01%). We obtained similarly high agreement between the 65 known locations of force application and the center of pressure measures obtained from the force treadmill, these were 2.5 and 2.8 mm in the x and y axes, respectively (comparison μ = 21.5 mm; min = 3.5 mm). Finally, the results from our additional crosstalk testing lend further support to the assessment of high accuracy for this device.

The dynamic testing which was conducted by administering over-ground and force treadmill sprints at the same speeds, extend the findings of other investigators, established at lesser speeds, that the

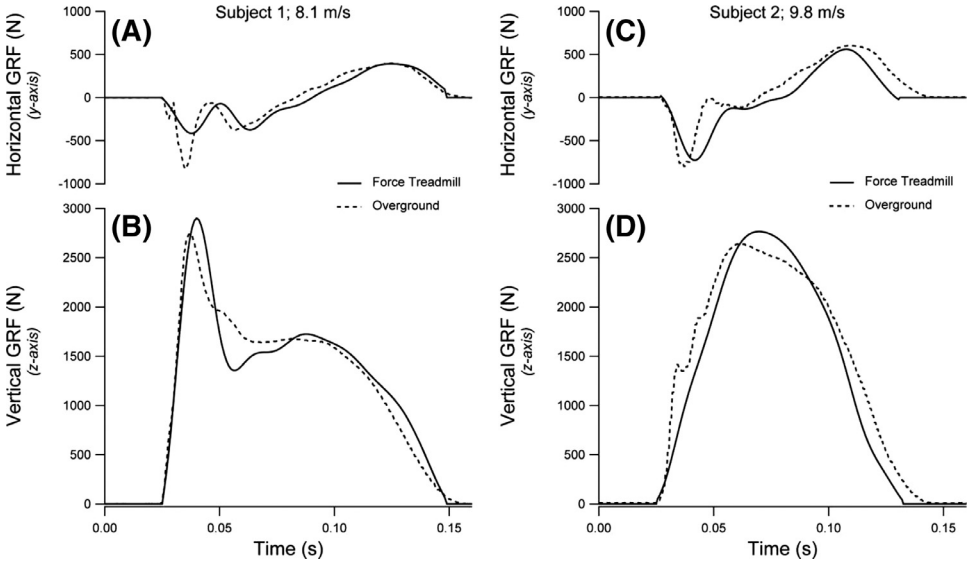

Fig. 4. Comparison of the horizontal (y axis; A and C) and vertical (z axis; B and D) ground reaction forces obtained for two subjects at their respective top speeds. The force platform data were conditioned with a 60 Hz notch filter. The force treadmill signals were chosen for match and conditioned with a dual-pass 6-pole Butterworth resulting in a zero-lag, low-pass filter with frequency cutoff of 40 Hz. The distinct patterns of vertical force application between the subjects are due to the foot strikes used; subject 1 used a heel-strike, subject 2 was a forefoot striker.

gait of individual's does not appear to vary appreciably when running over-ground or upon an instrumented force treadmill [1,7,30,31]. These data further indicate that our choice of post-acquisition filter routines for the reaction force data does not add unnecessary distortion to the measurements and maintains the subject specific characteristics of the foot ground collision evident in the high-speed running illustrated in Fig. 4.

Finally, we offer three suggestions for others contemplating the construction of a similar device. First, the instantaneous torques necessary to maintain a constant belt speed during the stance phase requires a powerful motor and an appropriate controller. Second, special consideration needs to be given to the position and routing of the data and power cables, because the low voltage signals traveling between the load cells and amplifier are highly susceptible to electromagnetic interference caused by the current flow to the motor. This contamination is best mitigated in the design stage rather than the post hoc treatments we used. Third, the numerous benefits of honeycomb composites account for their widespread use in construction requiring materials of high stiffness but low mass. However, for horizontal measurements it is important to align the ribbon of the internal core with the axis of desired stiffness because in general the non-ribbon orientation has stiffness characteristics that are roughly 50% of the ribbon direction [21].

Considerable success in revealing the physiology of animal design has come forth while studying locomotion and exercise at the limits of performance. In terrestrial gait, force application against the ground is the primary method of achieving increased performance and faster running speeds [26,32]. However, the gait and physiological mechanisms individuals use to apply force against the ground and how this variability influences performance has only recently been explored due to the unavailability of adequate measurement equipment [5,32]. We conclude this design provides a, precise, instrumented treadmill capable of recording multi-axis ground reaction forces applied during the foot ground contacts of the fastest men and animals known to science.

Conflicts of interest

The authors have none to declare.

Ethical approval

Data collection was approved by the University of Montana's Institutional Review Board with an internal reference number 85-14. The subjects volunteered and provided their written informed consent prior to participation.

Acknowledgments

We thank Drew Krutak, Eric McDonald, and Jeremy Hanneman for technical research on the feasibility of flexible line shafts. Chris Sundberg, Barney Conrad and Forrest Carignan provided assistance and advice with design, fabrication and welding. This work was supported by funds from the Dennis and Phyllis Washington Foundation and a graduate fellowship from the A.P. Sloan Foundation (MP).

References

[1] Kram R, Griffin TM, Donelan JM, Chang YH. Force treadmill for measuring vertical and horizontal ground reaction forces. J Appl Physiol 1998;85:764–9.
[2] Paolini G, Della Croce U, Riley PO, Newton FK, Casey Kerrigan D. Testing of a tri-instrumented-treadmill unit for kinetic analysis of locomotion tasks in static and dynamic loading conditions. Med Eng Phys 2007;29:404–11.
[3] Weyand PG, Bundle MW, McGowan CP, Grabowski A, Brown MB, Kram R, et al. The fastest runner on artificial legs: different limbs, similar function? J Appl Physiol 2009;107:903–11.
[4] McGowan CP, Grabowski AM, McDermott WJ, Herr HM, Kram R. Leg stiffness of sprinters using running-specific prostheses. J R Soc Interface 2012;9:1975–82.
[5] Clark KP, Weyand PG. Are running speeds maximized with simple-spring stance mechanics? J Appl Physiol 2014;117:604–15.
[6] Graubner R, Nixdorf E. Biomechanical analysis of the sprint and hurdles events at the 2009 IAAF World Championships in athletics. New Stud Athletics 2011;26:19–53.
[7] Moravec P, Ruzicka J, Susanka P, Dostal E, Kodejs M, Nosek M. The 1987 International Athletic Foundation/IAAF Scientific Project Report: time analysis of the 100 metres events at the II World Championships in Athletics. New Stud Athletics 1988;3:61–96.
[8] Draper ER. A treadmill-based system for measuring symmetry of gait. Med Eng Phys 2000;22:215–22.
[9] Riley PO, Dicharry J, Franz J, Croce UD, Wilder RP, Kerrigan DC. A Kinematics and kinetic comparison of overground and treadmill running. Med Sci Sports Exerc 2008;40:1093–100.
[10] Munro CF, Miller DI, Fuglevand AJ. Ground reaction forces in running: a reexamination. J Biomech 1987;20:147–55.
[11] Kram R, Powell A. A treadmill-mounted force platform. J Appl Physiol 1989;67:1692–8.

[12] Davis BL, Cavanagh PR. Decomposition of superimposed ground reaction forces into left and right force profiles. J Biomech 1993;26:593–7.
[13] Dingwell J, Davis B. A rehabilitation treadmill with software for providing real-time gait analysis and visual feedback. J Biomech Eng 1996;118:253–5.
[14] Belli A, Bui P, Berger A, Geyssant A, Lacour J-R. A treadmill ergometer for three-dimensional ground reaction forces measurement during walking. J Biomech 2001;34:105–12.
[15] Dierick F, Penta M, Renaut D, Detrembleur C. A force measuring treadmill in clinical gait analysis. Gait Posture 2004;20:299–303.
[16] Jansen EC, Vittas D, Hellberg S, Hansen J. Normal gait of young and old men and women: ground reaction force measurement on a treadmill. Acta Orthop 1982;53:193–6.
[17] Willems PA, Gosseye TP. Does an instrumented treadmill correctly measure the ground reaction forces? Biol Open 2013;2:1421–4.
[18] Heglund NC. A simple design for a force-plate to measure ground reaction forces. J Exp Biol 1981;93:333–8.
[19] Biewener AA, Full RJ. Force platform and kinematic analysis. Biomechanics—structures and systems: a practical approach. Biewener; 1992. p. 45–73.
[20] Weyand PG, Davis JA. Running performance has a structural basis. J Exp Biol 2005;208:2625–31.
[21] Hexcel. Honeycomb sandwich design technology, Duxford (UK): Hexcel Co., Ltd.; 2000. Publication No. AGU 075b.
[22] Bitzer T. Honeycomb technology: materials, design, manufacturing, applications and testing. London: Chapman & Hall; 1997.
[23] Robertson DGE, Dowling JJ. Design and responses of Butterworth and critically damped digital filters. J Electromyogr Kinesiol 2003;13:569–73.
[24] Hedrick TL. Software techniques for two-and three-dimensional kinematic measurements of biological and biomimetic systems. Bioinspir Biomim 2008;3:034001.
[25] Bundle MW, Hoyt RW, Weyand PG. High-speed running performance: a new approach to assessment and prediction. J Appl Physiol 2003;95:1955–62.
[26] Weyand PG, Sternlight DB, Bellizzi MJ, Wright S. Faster top running speeds are achieved with greater ground forces not more rapid leg movements. J Appl Physiol 2000;89:1991–9.
[27] Collins SH, Adamczyk PG, Ferris DP, Kuo AD. A simple method for calibrating force plates and force treadmills using an instrumented pole. Gait Posture 2009;29:59–64.
[28] Paolini G, Della Croce U, Riley PO, Newton FK, Kerrigan C. Testing of a tri-instrumented-treadmill unit for kinetic analysis of locomotion tasks in static and dynamic loading conditions. Med Eng Phys 2007;29:404–11.
[29] Verkerke GJ, Hof AL, Zijlstra W, Ament W, Rakhorst G. Determining the centre of pressure during walking and running using an instrumented treadmill. J Biomech 2005;38:1881–5.
[30] van Ingen Schenau GJ. Some fundamental aspects of the biomechanics of over-ground versus treadmill locomotion. Med Sci Sports Exerc 1980;12:257–61.
[31] Williams KR. Biomechanics of running. Exerc Sport Sci Rev 1985;13:389–441.
[32] Weyand PG, Sandell RF, Prime DN, Bundle MW. The biological limits to running speed are imposed from the ground up. J Appl Physiol 2010;108:950–61.